Composites Communications 26 (2021) 100775

Contents lists available at ScienceDirect

Composites Communications

journal homepage: www.elsevier.com/locate/coco

Engineered/strain-hardening cementitious composites (ECC/SHCC) with an ultra-high compressive strength over 210 MPa

Bo-Tao Huang [a], Ke-Fan Weng [a,b], Ji-Xiang Zhu [a], Yu Xiang [a,**], Jian-Guo Dai [a,*], Victor C. Li [c]

[a] Department of Civil and Environmental Engineering, The Hong Kong Polytechnic University, Kowloon, Hong Kong, China
[b] Department of Ocean Science and Engineering, Southern University of Science and Technology, Shenzhen, Guangdong, China
[c] Department of Civil and Environmental Engineering, University of Michigan, Ann Arbor, USA

ARTICLE INFO

Keywords:
Engineered cementitious composites (ECC)
Strain-hardening cementitious composites (SHCC)
Ultra-high performance concrete (UHPC)
Ultra-high strength
Hybrid fiber reinforcement

ABSTRACT

Engineered/Strain-Hardening Cementitious Composites (ECC/SHCC) are fiber-reinforced cement-based materials with tensile strain-hardening and multiple-cracking characteristics. In this study, ultra-high-strength ECC (UHS-ECC) with a compressive strength over 210 MPa was successfully developed for the first time. The developed UHS-ECC exhibited excellent tensile strain capacity (5.2%), and fine crack width (72 μm). These characteristics were realized by combined use of polyethylene and steel fibers in a dense matrix. Two new material indices ($f'_c f_t \varepsilon_t$ index and $f'_c f_t \varepsilon_t / w$ index) were proposed to assess the overall performance of UHS-ECC. Compared with existing high-strength ECC, the developed UHS-ECC records the highest compressive strength and the best overall performance. The findings of this study provide useful knowledge for future design and applications of UHS-ECC.

1. Introduction

Engineered Cementitious Composites (ECC) are fiber-reinforced cement-based materials with tensile strain-hardening and multiple-cracking characteristics (typically crack width < 100 μm) [1–3]. This material is designed based on micromechanical principles [4–5] and is also popularly known as strain-hardening cementitious composites (SHCC) [6–8] or ultra-high toughness cementitious composites (UHTCC) [9–10]. For ordinary ECC, the compressive strength ranges from 20 to 80 MPa [11,12] and the tensile strain capacity ranges from 2% to 8% [1,3]. Compared with conventional fiber-reinforced concrete [13], ECC shows superior mechanical performance and crack-control behavior under monotonic and cyclic loadings [14–17]. ECC has excellent durability performance even under a cracked state [18–20], owing to its fine crack width and self-healing characteristics. Thus, ECC is considered as an ideal material for strengthening and repair, and for new construction of transport, hydraulic, and marine infrastructures that are subjected to complex loading conditions and severe service environments [1,21–23].

For fiber-reinforced cementitious composites, a high-strength matrix with dense microstructure is beneficial for their stiffness and durability performance in practical applications. Hence, in recent years, high-strength ECC with a compressive strength over 100 MPa and a tensile strain capacity of 2%–11% [24–37] has been developed. For example, the high-strength ECC developed by Ranade [26] showed the highest compressive strength (205 MPa), while the others showed a compressive strength lower than 170 MPa. It is noted that the ECC with 205 MPa compressive strength exhibited a relatively large crack width (i.e., 135 μm) under tensile loading [26]. For ECC materials, a finer crack width (typically < 100 μm) has been shown critical for its self-healing and durability performance [38]. It is therefore highly desirable to develop an ECC material with ultra-high strength, excellent ductility and very fine crack width. However, the existing knowledge in this aspect remains limited.

This study aimed at developing an ultra-high strength ECC (UHS-ECC) with a compressive strength over 200 MPa, a tensile strain capacity over 5%, and a crack width below 100 μm. The mechanical properties of the developed UHS-ECC were investigated in terms of the compressive strength, tensile strength, tensile strain capacity, crack pattern, and crack width, using existing high-strength ECCs as a benchmark. The fiber failure modes on the tensile fracture surface were analyzed to gain a better understanding of the achieved mechanical properties of UHS-ECC.

* Corresponding author.
** Corresponding author.
E-mail addresses: botaohuang@zju.edu.cn (B.-T. Huang), ke-fan.weng@connect.polyu.hk (K.-F. Weng), ji-xiang.zhu@connect.polyu.hk (J.-X. Zhu), cee.yu.xiang@polyu.edu.hk (Y. Xiang), cejgdai@polyu.edu.hk (J.-G. Dai), vcli@umich.edu (V.C. Li).

https://doi.org/10.1016/j.coco.2021.100775
Received 4 January 2021; Received in revised form 26 April 2021; Accepted 26 April 2021
Available online 8 May 2021

Table 1
Mix proportions (kg/m^3).

Raw material	M-P2.0S1.0	M-P1.5S1.5
Cement	1126	1126
Silica fume (SF)	282	282
Slag	141	141
Quartz powder (QP)	141	141
Silica sand	422	422
Water	245	245
Superplasticizer (in solid)	23	23
PE fiber (Vol %)	2.0%	1.5%
Steel fiber (Vol %)	1.0%	1.5%

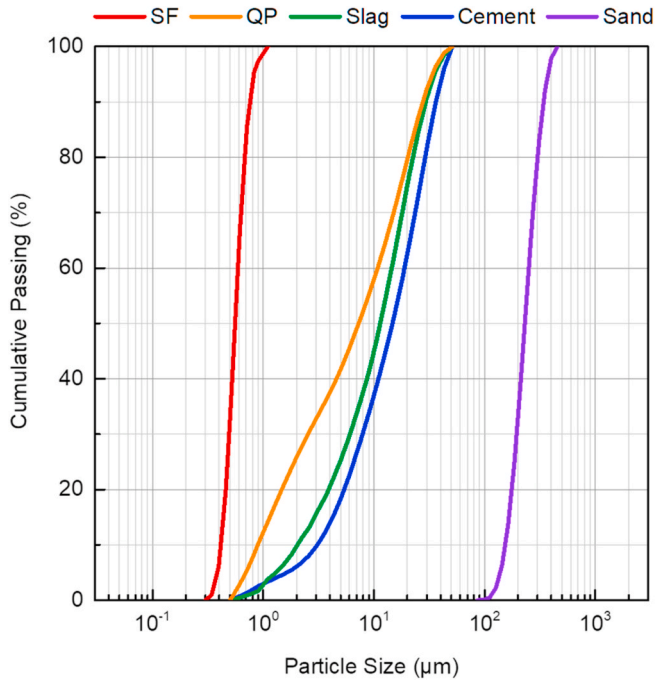

Fig. 1. Particle size distributions of raw materials.

Table 2
Properties of PE and steel fibers (obtained from the suppliers).

Fiber	Diameter (μm)	Length (mm)	Strength (MPa)	Modulus (GPa)	Density (g/cm^3)
PE fiber	24	12	3000	100	0.97
Steel fiber	200	13	≥2000	210	7.8

2. Experimental program

2.1. Raw materials and mix proportions

Mix proportions. The UHS-ECC mixtures studied are presented in Table 1. The main difference between the two mixes was the fiber content. The cement was Type I 52.5 N Portland cement (BS EN 197–1:2011). The particle size distributions of cement, silica fume (SF), slag, quartz powder (QP), and silica sand are presented in Fig. 1. The maximum particle sizes of cement, silica fume, and slag were no more than 50 μm, the mean particle size of the quartz powder was 7.5 μm, and the mean particle size of the silica sand was below 300 μm. Polycarboxylate ether superplasticizer (SP) was used for water reduction. In both mixes, polyethylene (PE) fiber and steel fiber were used together. For the UHS-ECC matrix, the water-to-binder (cement, silica fume, and slag) ratio was 0.158, the sand to binder ratio was 0.272, and the SP to binder ratio was 0.0148. The cementitious paste volume (the volumetric ratio of paste in one cubic meter) is important for the performance of cement-based materials [39]. For the UHS-ECC, the paste volume was approximately 0.8. It is noted that lower sand volume (i.e., higher paste volume) can lead to lower fracture toughness of matrix, which is desirable for tensile strain-hardening behavior. Hence, a comparatively high paste volume (i.e., 0.8) was used for UHS-ECC in this study.

Fibers. Table 2 lists the properties of PE and steel fibers. The PE fiber has diameter and length of 24 μm and 12 mm, respectively. The straight steel fiber has diameter and length of 200 μm and 13 mm, respectively. Generally, 1.5–2.0% (Vol.) PE fibers are used for high-strength ECC [3,25,28,30], and 1–4% (Vol.) steel fibers are used for ultra-high performance concrete (UHPC) [40–43]. In addition, the hybrid use of steel and synthetic fibers can improve the compressive strength of both normal- and high-strength ECC [44,45]. For the UHS-ECC, hybrid fiber reinforcement (PE and steel fibers) was used.

Chemical compositions. The chemical compositions of the cement, silica fume, slag, and quartz powder, analyzed by X-ray fluorescence (XRF) spectroscopy (Bruker AXS GmbH), are presented in Table 3. The content of silica dioxide in the silica fume was over 93% (by mass).

2.2. Material preparation and testing methods

Material preparation. The mixing process of UHS-ECC was as follows: (a) the cement, silica fume, slag, quartz powder and silica sand were mixed for 2–3 min; (b) the water and superplasticizer were added and mixed for 10–12 min; (c) the PE and steel fibers were added and mixed for 5–6 min; (d) the prepared mixture was cast into molds. According to ASTM C1437 [46], the mini-slump spread diameters of M-P2.0S1.0 and M-P1.5S1.5 were 129 mm and 138 mm, respectively. Generally, the spread diameters of normal ECC, high-strength ECC, and UHPC are 250–350 mm [47], 160–180 mm [23], and 200–250 mm [48], respectively. Compared with these materials, UHS-ECC showed significantly lower flowability. Thus, more efforts are needed to improve the workability of UHS-ECC in future study.

Curing procedure. The cast UHS-ECC was stored at 20 °C for 24 h, demolded and cured in 90 °C water for 9 d to accelerate the hydration reaction [25,26]. After heat curing, UHS-ECC was placed in a lab environment (room temperature: 20–24 °C). In this study, all mechanical properties of UHS-ECC were tested at 12 d after casting.

Compression test. Three 50 mm × 50 mm × 50 mm cubes were prepared for each mix, according to ASTM C109/C109 M [49]. It is noted that this cube specimen has been used to evaluate the compressive strength of high-strength ECC in many existing studies (e.g. Refs. [3,25,26,28,32,34]). Hence, for comparison, this specimen was also used for UHS-ECC. As the strength measured by standard concrete cube and prism should be more convincing, additional compressive tests are needed for UHS-ECC in future study. The elastic modulus of UHS-ECC

Table 3
Chemical compositions of cement, silica fume, slag, and quartz powder.

Raw material	SiO_2	Fe_2O_3	Al_2O_3	CaO	TiO_2	SO_3	P_2O_5	MgO	K_2O	ZrO_2	Cl
Cement	22.60	0.21	4.27	67.10	0.12	3.96	0.13	1.03	0.19	/	0.08
Silica fume	93.20	0.41	0.80	0.10	0.07	0.08	0.31	/	0.10	4.50	0.01
Slag	31.80	0.72	18.90	35.5	0.8	2.35	0.11	8.69	0.57	0.05	0.04
Quartz powder	96.40	0.14	0.74	0.81	/	0.90	0.12	0.10	0.61	/	0.13

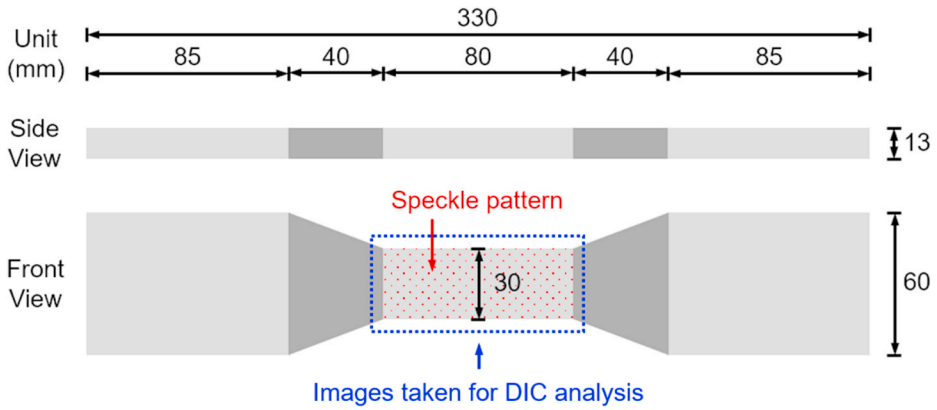

Fig. 2. Dimensions of the specimen for direct tension test.

Table 4
Mechanical proportions of UHS-ECC.

Proportions	M-P2.0S1.0	M-P1.5S1.5
Compressive strength (MPa)	210.6 ± 4.7	213.2 ± 2.0
Tensile strength (MPa)	16.1 ± 0.9	15.6 ± 0.5
Tensile strain capacity (%)	5.2 ± 0.8	3.4 ± 0.4
Average crack width at the ultimate tensile strain (μm)	71.7 ± 2.5	112.3 ± 9.7
Elastic modulus (GPa)	52.5 ± 0.9	52.9 ± 0.3

was measured using a cylinder specimen (Φ75 mm × 150 mm) according to ASTM C469/C469 M [50].

Direct tension test. According to Ref. [51], three dumbbell samples were prepared for each mix (Fig. 2). The loading rate was set to 0.5 mm/min [51], and the tensile deformation of the central part (80 mm length) was measured using a linear variable differential transformer (LVDT). To monitor the strain field of UHS-ECC, digital image correlation (DIC) was applied to analyze the cracking behavior of ECC materials [52,53]. The speckle pattern for DIC analysis was applied on the middle part of the specimen (Fig. 2). During the test, digital images were captured every 3 s.

Scanning electron microscopy (SEM). After the direct tension test, the fiber failure modes on the fracture surface of UHS-ECC were investigated using SEM (Jeol 6490).

3. Test results and discussions

3.1. Mechanical properties of UHS-ECC

The mechanical properties of the developed UHS-ECC are summarized in Table 4. For both UHS-ECC mixes, the compressive strength was over 210 MPa (210.6 MPa for M-P2.0S1.0 and 213.2 MPa for M-P1.5S1.5). The elastic moduli of M-P2.0S1.0 and M-P1.5S1.5 were 52.5 GPa and 52.9 GPa respectively. The tensile stress–strain relations (Fig. 3) showed clear strain-hardening behavior. M-P2.0S1.0 achieved an average tensile strength of 16.1 MPa and an average strain capacity of 5.2% (i.e., approximately 520 times that of ordinary concrete). M-P1.5S1.5 achieved an average tensile strength of 15.6 MPa and an average strain capacity of 3.4% (i.e., approximately 340 times that of ordinary concrete). It is noted that the ratio between compressive strength and tensile strength of UHS-ECC was less than 1/10, indicating that further improvement of the tensile strength is needed. According to the design theory of ECC [1], the tensile strength depends on fiber aspect ratio, fiber content, and fiber/matrix bond strength. For the UHS-ECC, there is very limited room to improve the fiber content, as 3% (Vol.) fiber was already used. Thus, it is desirable to adjust the fiber aspect ratio and to improve the fiber/matrix bond (e.g., using surface treatment technology) in following study.

The average crack width for each group is listed in Table 4. According to the method in Ref. [37], the crack width was calculated based

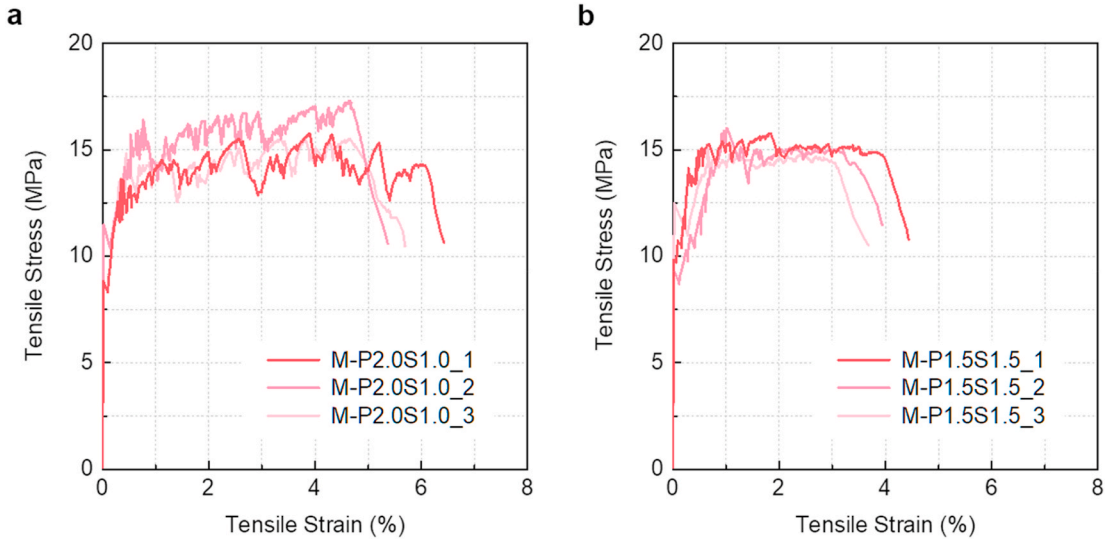

Fig. 3. Tensile stress–strain relations of UHS-ECC: (a) M-P2.0S1.0 and (b) M-P1.5S1.5. M-P2.0S1.0 has a tensile strength of 16.1 MPa and a strain capacity of 5.2%, and M-P1.5S1.5 has a tensile strength of 15.6 MPa and a strain capacity of 3.4%.

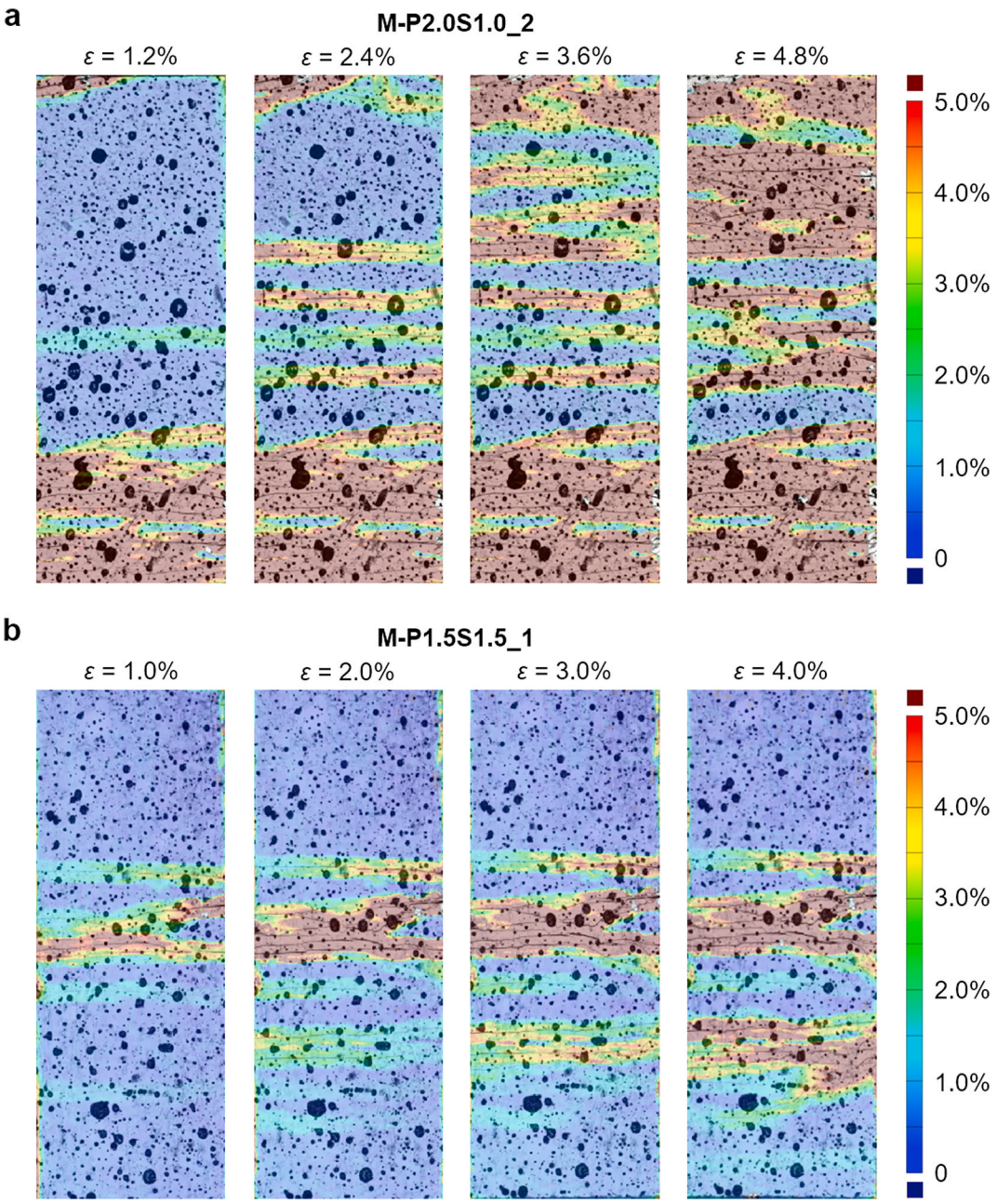

Fig. 4. DIC strain fields and crack patterns of the typical samples at different strain levels: (a) M-P2.0S1.0 and (b) M-P1.5S1.5. Significant multiple cracking can be observed for both materials. Color code shows local tensile strain values. (For interpretation of the references to colour in this figure legend, the reader is referred to the Web version of this article.)

on the original high-resolution digital image taken at the ultimate tensile strain of each sample. The average crack widths of M-P2.0S1.0 and M-P1.5S1.5 were found to be 72 μm and 112 μm, respectively, even under the ultimate tensile strain levels (i.e., 5.2% for M-P2.0S1.0 and 3.4% for M-P1.5S1.5). It is expected that the crack widths under the service condition are much smaller, which is critical for the durability performance of UHS-ECC. The first cracking strains of the UHS-ECC were approximately 0.018–0.025%. Overall, the cracking strains of M-P2.0S1.0 and M-P1.5S1.5 were close, because the difference of the fiber reinforcement in two mixes were not significant.

It is known that UHPC has ultra-high strength (typically $\geq$ 150 MPa in compression) with specified durability and tensile ductility [40,42,54,55]. In this respect, the UHS-ECC developed can be considered as a specific type of UHPC, and hence can also be named as ultra-high performance ECC (UHP-ECC).

3.2. DIC strain fields and crack patterns

Fig. 4 presents the DIC strain fields and crack patterns of two typical samples (M-P2.0S1.0_2 and M-P1.5S1.5_1) at four strain levels ($0.25\varepsilon_t$, $0.5\varepsilon_t$, $0.75\varepsilon_t$, and ε_t). Here, ε_t is the tensile strain capacity of the sample. It is noted that the crack patterns of the samples in each group were similar, and the typical samples were selected based on the quality of the digital photographs, which is important for a reliable DIC analysis. In Fig. 4, significant multiple cracking can be observed for both materials. As the tensile strain increased, the number of cracks in UHS-ECC increased. It can be also seen that at the ultimate stage, the crack number of M-P2.0S1.0_2 was significantly larger than that of M-P1.5S1.5_1, leading to the higher tensile strain capacity of the former. In addition, almost saturated multiple cracking was achieved in M-P2.0S1.0_2, while the cracks of M-P2.0S1.0_1 were concentrated in the

Table 5
Summary of the mechanical properties of high-strength ECC in literature.

Material ID	f'_c (MPa)	ε_t (%)	f_t (MPa)	w (μm)	$f'_c\varepsilon_t$ Index (MPa)	$f'_cf_t\varepsilon_t$ Index (MPa^2)	$f'_cf_t\varepsilon_t/w$ Index (MPa^2/μm)
M-P2.0S1.0 (This study)	**211**	**5.2**	**16.1**	**72**	**10.9**	**175.5**	**2.45**
M-P1.5S1.5 (This study)	**213**	**3.4**	**15.6**	**112**	**7.3**	**114.6**	**1.02**
A (Kamal et al., 2008 [24])	96	2.8	10.0	61*	2.7	26.9	0.44
B (Ranade et al., 2013 [25])	166	3.4	14.5	180	5.6	81.8	0.45
C (Ranade 2014 [26])	205	4.6	16.1	135	9.4	151.3	1.12
D (Curosu et al., 2017 [27])	134	3.9	7.6	68*	5.2	39.6	0.58
E (He et al., 2017 [28])	153	2.3	15.0	71	3.5	52.8	0.74
F (Chen et al., 2018 [29])	150	2.4	10.8	48*	3.6	38.9	0.81
G (Yu et al., 2018 [30])	122	8.2	17.4	160*	9.9	172.9	1.08
H (Lei et al., 2019 [31])	163	6.5	7.0	85	10.6	74.5	0.88
I (Lu et al., 2019 [32])	132	6.4	10.4	58	8.4	87.9	1.52
J (Zhang et al., 2019 [33])	87	7.0	10.9	69	6.0	65.8	0.95
K (Li et al., 2020 [34])	131	11.0	12.1	138	14.4	174.0	1.26
L (Nguyễn et al., 2020 [35])	104	5.3	8.0	83	5.4	43.5	0.53
M (Zhang et al., 2020 [36])	109	3.8	13.0	78	4.2	54.4	0.70
N (Huang et al., 2021 [37])	134	7.0	7.1	86	9.4	66.6	0.77

Note: * represents that this value was estimated based on the data in the corresponding reference.

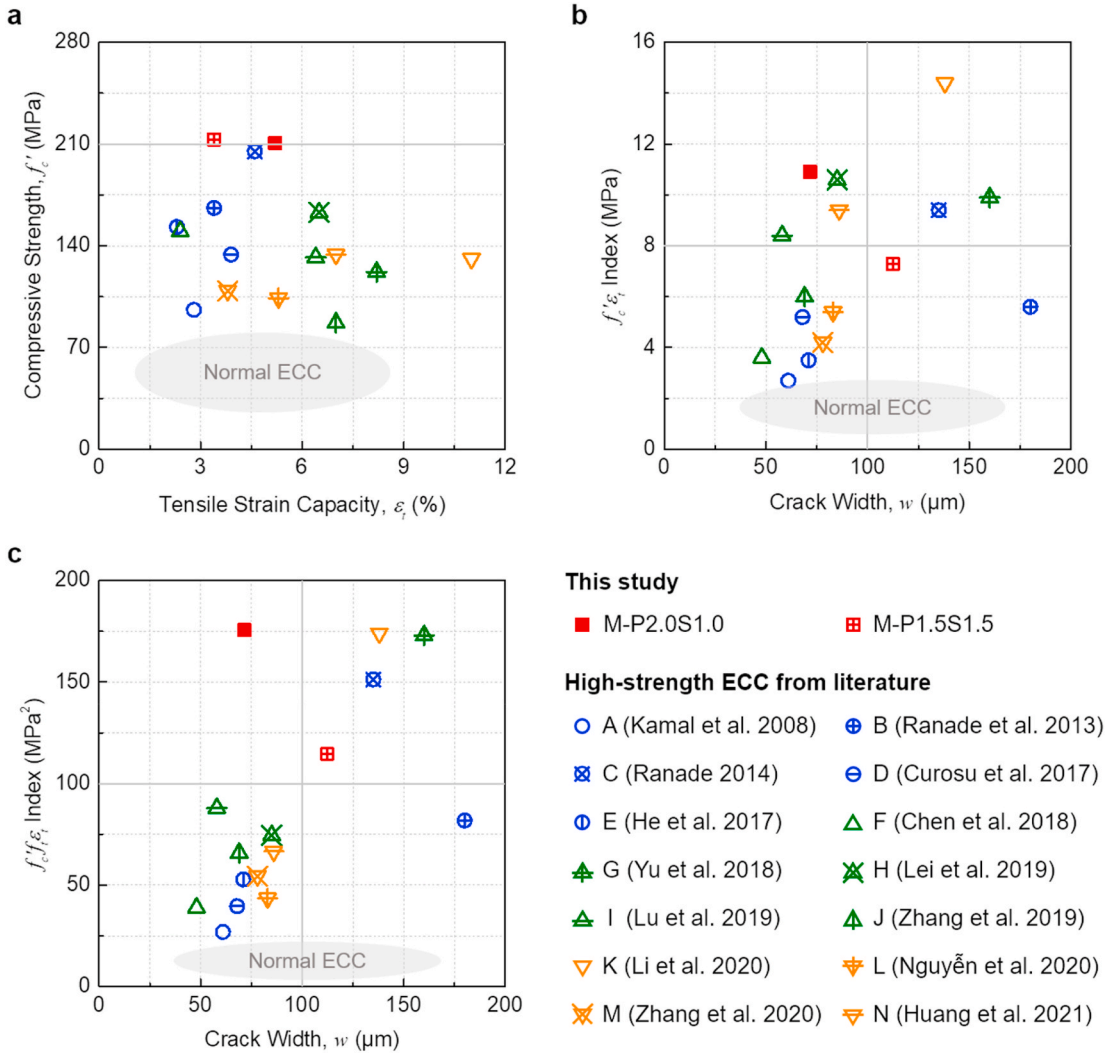

Fig. 5. Comparison between UHS-ECC and existing high-strength ECC: (a) compress strength *vs.* tensile strain capacity relation, (b) $f'_c\varepsilon_t$ index *vs.* crack width relation, and (c) $f'_cf_t\varepsilon_t$ index *vs.* crack width relation. Compared with high-strength ECC in literature, the developed UHS-ECC (M-P2.0S1.0) shows the best overall performance.

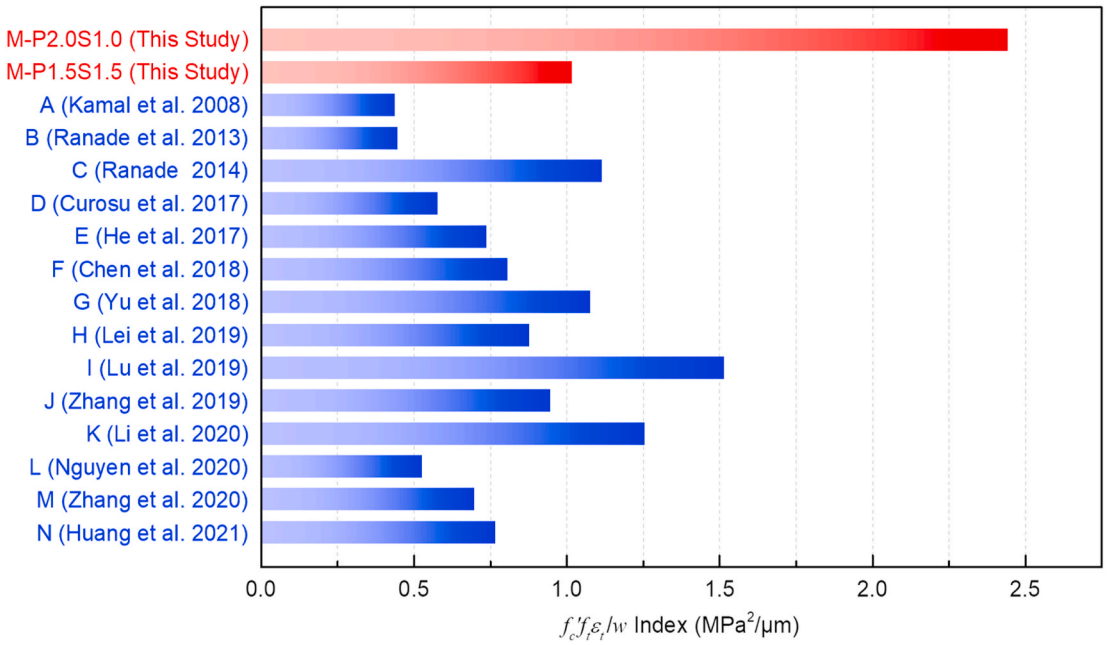

Fig. 6. $f'_c f_t \varepsilon_t / w$ indices of UHS-ECC and existing high-strength ECC. Compared with high-strength ECC in literature, the developed UHS-ECC (M-P2.0S1.0) shows the highest $f'_c f_t \varepsilon_t / w$ index.

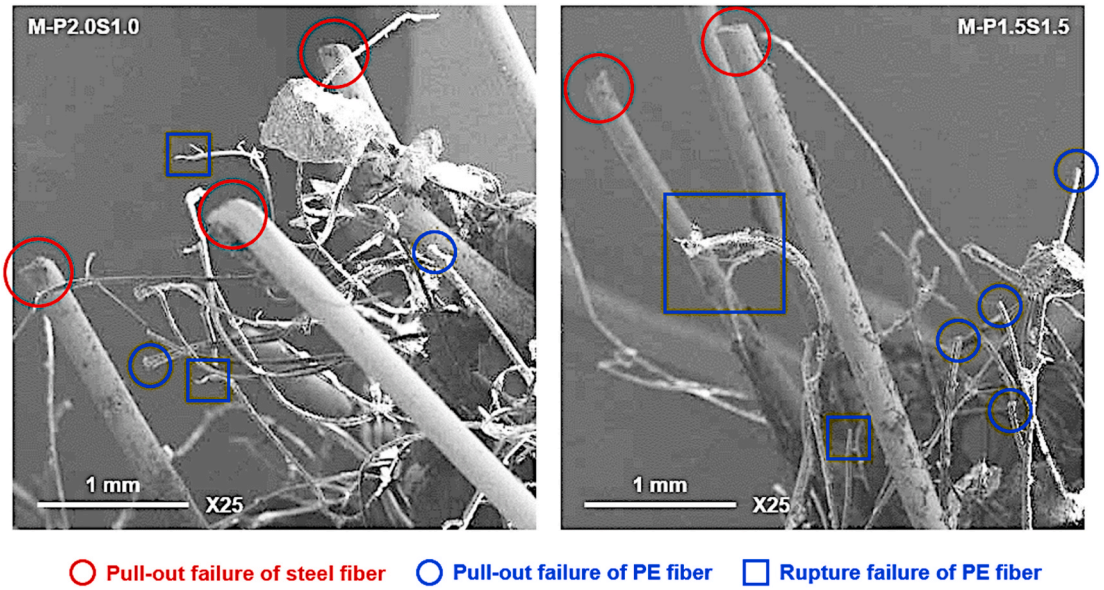

Fig. 7. Fiber failure modes of M-P2.0S1.0 and M-P1.5S1.5. For the steel fibers, pull-out ends can be observed. For the PE fibers, both rupture and pull-out ends can be observed.

lower half of the tension zone.

3.3. Comparison between UHS-ECC and existing high-strength ECC

Table 5 summarizes the mechanical properties of the high-strength ECC reported in the literature. Here, f'_c is the compressive strength, f_t is the tensile strength, ε_t is the tensile strain capacity, and w is the average crack width at the ultimate tensile strain. To evaluate the compressive strength and tensile ductility together, the $f'_c\varepsilon_t$ index was used, which is defined as the product of compressive strength and tensile strain capacity (i.e., $f'_c \times \varepsilon_t$) [26]. Also, the tensile strength and crack width of ECC are critical for practical applications. Thus, two new indices ($f'_c f_t \varepsilon_t$ index and $f'_c f_t \varepsilon_t / w$ index) are proposed. The $f'_c f_t \varepsilon_t$ index, defined as $f'_c \times f_t \times \varepsilon_t$, can be used to evaluate the compressive strength, tensile strength, and tensile ductility together. As a smaller crack width (w) is beneficial to the durability of ECC, the reciprocal of w is used in the $f'_c f_t \varepsilon_t / w$ index. Note that for $f'_c\varepsilon_t$, $f'_c f_t \varepsilon_t$ and $f'_c f_t \varepsilon_t / w$ indices, the larger the value, the better the performance. For comparison, the values of these indices are collected in Table 5 for each material.

Fig. 5 compares the developed UHS-ECC and existing high-strength ECC, including the compressive strength *vs.* tensile strain capacity relation (Fig. 5a), the $f'_c\varepsilon_t$ index *vs.* crack width relation (Fig. 5b), and the $f'_c f_t \varepsilon_t$ index *vs.* crack width relation (Fig. 5c). In Fig. 5a, it is evident that the UHS-ECC materials (M-P2.0S1.0 and M-P1.5S1.5) have the highest compressive strength. The properties of normal ECC are included in Fig. 5a for comparison. In Fig. 5b, only four reported mixes

achieved an $f'_c\varepsilon_t$ index over 8 MPa and a crack width below 100 μm, and M-P2.0S1.0 in the present study shows the highest $f'_c\varepsilon_t$ index (10.9 MPa) compared with the other three. In Fig. 5c, M-P2.0S1.0 is the only material having an $f'_cf_t\varepsilon_t$ index over 100 MPa^2 and a crack width below 100 μm. Additionally, the $f'_cf_t\varepsilon_t/w$ index of M-P2.0S1.0 is the highest among all reported materials (Fig. 6). According to Figs. 5 and 6, it is concluded that the developed UHS-ECC (M-P2.0S1.0) shows the best overall performance, as compared with other high-strength ECC materials in the literature.

3.4. SEM observation for fiber failure modes

The SEM images of the fiber failure modes of M-P2.0S1.0 and M-P1.5S1.5 are presented in Fig. 7. It can be observed that for both UHS-ECC, the PE fibers exhibited a combination of pull-out and rupture failure, while all steel fibers were pulled out. The dense UHS-ECC matrix resulted in a strong fiber/matrix bond leading to the rupture of the PE fibers with long embedment lengths. Compared with the PE fibers, the steel fibers with higher strength and diameter can sustain a larger rupture force, so that only pull-out failure occurred. The rupture of some PE fibers indicates that the fiber strength is effectively utilized in UHS-ECC due to improved fiber/matrix interfacial bond [23,37].

4. Conclusions

In this study, ultra-high strength engineered cementitious composites (UHS-ECC) with compressive strength over 210 MPa were successfully developed for the first time through the hybrid use of PE fiber and steel fiber in combination with a dense reactive matrix. This research demonstrates that UHS-ECC with high tensile strain capacity in excess of 5% and an average crack width below 80 μm is achievable. Two new indices ($f'_cf_t\varepsilon_t$ index and $f'_cf_t\varepsilon_t/w$ index) were proposed to evaluate the overall performance of strain-hardening cement-based materials. Compared with existing high-strength ECC materials, the developed UHS-ECC showed the highest compressive strength and the best overall performance. The SEM observation of partial PE fiber rupture suggests efficient use of high strength fibers in UHS-ECC. The successful development of UHS-ECC provides a potent platform for the advancement of infrastructure with extreme durability and resiliency.

Further study is being conducted to achieve a comprehensive understanding of the influence of fiber hybridization and aspect ratios on the mechanical properties of UHS-ECC. As fiber reinforcement can improve the bond between rebar and concrete [56], it is also desirable to investigate the bond between rebar and UHS-ECC, which is meaningful for practical applications.

CRediT authorship contribution statement

Bo-Tao Huang: Conceptualization, Methodology, Investigation, Visualization, Writing – original draft. **Ke-Fan Weng:** Investigation, Validation. **Ji-Xiang Zhu:** Investigation, Data curation. **Yu Xiang:** Formal analysis, Data curation, Writing – review & editing. **Jian-Guo Dai:** Conceptualization, Funding acquisition, Supervision, Writing – review & editing. **Victor C. Li:** Supervision, Writing – review & editing.

Declaration of competing interest

The authors declare that they have no known competing financial interests or personal relationships that could have appeared to influence the work reported in this paper.

Acknowledgments

This study was supported by financial support received from Chinese Guangdong Province R&D Plan for Key Areas (2019B111107002), Hong Kong General Research Fund (RGC) (No. 15214517) and the Hong Kong Innovation and Technology Fund (No. ITS/077/18FX). Bo-Tao Huang acknowledges the support by The Hong Kong Polytechnic University through the Research Institute for Sustainable Urban Development (No.1-BBWE) and the Postdoctoral Fellowships Scheme (No. YW4K).

References

[1] V.C. Li, Engineered Cementitious Composites (ECC) - Bendable Concrete for Sustainable and Resilient Infrastructure, Verlag GmbH Germany: Springer, Berlin, Heidelberg, 2019.
[2] V.C. Li, S. Wang, C. Wu, Tensile strain-hardening behavior of polyvinyl alcohol engineered cementitious composite (PVA-ECC), ACI Mater. J. 98 (6) (2001) 483–492.
[3] B.T. Huang, J. Yu, J.Q. Wu, J.G. Dai, C.K. Leung, Seawater sea-sand Engineered Cementitious Composites (SS-ECC) for marine and coastal applications, Compos. Commun. 20 (2020), 100353.
[4] V.C. Li, C.K.Y. Leung, Steady-state and multiple cracking of short random fiber composites, J. Eng. Mech. 118 (11) (1992) 2246–2264.
[5] C.K.Y. Leung, Design criteria for pseudoductile fiber-reinforced composites, J. Eng. Mech. 122 (1) (1996) 10–18.
[6] S. Qian, J. Zhou, M.R. De Rooij, E. Schlangen, G. Ye, K. Van Breugel, Self-healing behavior of strain hardening cementitious composites incorporating local waste materials, Cement Concr. Compos. 31 (9) (2009) 613–621.
[7] J. Yu, C.K. Leung, Strength improvement of strain-hardening cementitious composites with ultrahigh-volume fly ash, J. Mater. Civ. Eng. 29 (9) (2017), 05017003.
[8] B.T. Huang, Q.H. Li, S.L. Xu, L. Zhang, Static and fatigue performance of reinforced concrete beam strengthened with strain-hardening fiber-reinforced cementitious composite, Eng. Struct. 199 (2019), 109576.
[9] Q.H. Li, B.T. Huang, S.L. Xu, Development of assembled permanent formwork using ultra high toughness cementitious composites, Adv. Struct. Eng. 19 (7) (2016) 1142–1152.
[10] B.T. Huang, Q.H. Li, S.L. Xu, W. Liu, H.T. Wang, Fatigue deformation behavior and fiber failure mechanism of ultra-high toughness cementitious composites in compression, Mater. Des. 157 (2018) 457–468.
[11] J. Zhou, J. Pan, C.K. Leung, Mechanical behavior of fiber-reinforced engineered cementitious composites in uniaxial compression, J. Mater. Civ. Eng. 27 (1) (2015), 04014111.
[12] B.T. Huang, Q.H. Li, S.L. Xu, B.M. Zhou, Frequency effect on the compressive fatigue behavior of ultrahigh toughness cementitious composites: experimental study and probabilistic analysis, J. Struct. Eng. 143 (8) (2017), 04017073.
[13] B. Ali, L.A. Qureshi, R. Kurda, Environmental and economic benefits of steel, glass, and polypropylene fiber reinforced cement composite application in jointed plain concrete pavement, Compos. Commun. 22 (2020), 100437.
[14] P. Jun, V. Mechtcherine, Behaviour of strain-hardening cement-based composites (SHCC) under monotonic and cyclic tensile loading: part 1–experimental investigations, Cement Concr. Compos. 32 (10) (2010) 801–809.
[15] F. Yuan, J. Pan, L. Dong, C.K.Y. Leung, Mechanical behaviors of steel reinforced ECC or ECC/concrete composite beams under reversed cyclic loading, J. Mater. Civ. Eng. 26 (8) (2014), 04014047.
[16] B.T. Huang, Q.H. Li, S.L. Xu, B.M. Zhou, Tensile fatigue behavior of fiber-reinforced cementitious material with high ductility: experimental study and novel PSN model, Construct. Build. Mater. 178 (2018) 349–359.
[17] B.T. Huang, Q.H. Li, S.L. Xu, Fatigue deformation model of plain and fiber-reinforced concrete based on Weibull function, J. Struct. Eng. 145 (1) (2019), 04018234.
[18] M. Şahmaran, V.C. Li, Durability of mechanically loaded engineered cementitious composites under highly alkaline environments, Cement Concr. Compos. 30 (2) (2008) 72–81.
[19] M. Şahmaran, V.C. Li, Durability properties of micro-cracked ECC containing high volumes fly ash, Cement Concr. Res. 39 (11) (2009) 1033–1043.
[20] H. Liu, Q. Zhang, V. Li, H. Su, C. Gu, Durability study on engineered cementitious composites (ECC) under sulfate and chloride environment, Construct. Build. Mater. 133 (2017) 171–181.
[21] K. Rokugo, T. Kanda, H. Yokota, N. Sakata, Applications and recommendations of high performance fiber reinforced cement composites with multiple fine cracking (HPFRCC) in Japan, Mater. Struct. 42 (9) (2009) 1197.
[22] B.T. Huang, Q.H. Li, S.L. Xu, B. Zhou, Strengthening of reinforced concrete structure using sprayable fiber-reinforced cementitious composites with high ductility, Compos. Struct. 220 (2019) 940–952.
[23] B.T. Huang, J.Q. Wu, J. Yu, J.G. Dai, C.K. Leung, High-strength seawater sea-sand Engineered Cementitious Composites (SS-ECC): mechanical performance and probabilistic modeling, Cement Concr. Compos. 114 (2020), 103740.
[24] A. Kamal, M. Kunieda, N. Ueda, H. Nakamura, Evaluation of crack opening performance of a repair material with strain hardening behavior, Cement Concr. Compos. 30 (10) (2008) 863–871.
[25] R. Ranade, V.C. Li, M.D. Stults, W.F. Heard, T.S. Rushing, Composite properties of high-strength, high-ductility concrete, ACI Mater. J. 110 (4) (2013) 413–422.
[26] R. Ranade, Advanced Cementitious Composite Development for Resilient and Sustainable Infrastructure, Ph.D. Thesis, University of Michigan, 2014.
[27] I. Curosu, M. Liebscher, V. Mechtcherine, C. Bellmann, S. Michel, Tensile behavior of high-strength strain-hardening cement-based composites (HS-SHCC) made with high-performance polyethylene, aramid and PBO fibers, Cement Concr. Res. 98 (2017) 71–81.

[28] S. He, J. Qiu, J. Li, E.H. Yang, Strain hardening ultra-high performance concrete (SHUHPC) incorporating CNF-coated polyethylene fibers, Cement Concr. Res. 98 (2017) 50–60.
[29] Y. Chen, J. Yu, C.K. Leung, Use of high strength strain-hardening cementitious composites for flexural repair of concrete structures with significant steel corrosion, Construct. Build. Mater. 167 (2018) 325–337.
[30] K.Q. Yu, J.T. Yu, J.G. Dai, Z.D. Lu, S.P. Shah, Development of ultra-high performance engineered cementitious composites using polyethylene (PE) fibers, Construct. Build. Mater. 158 (2018) 217–227.
[31] D.Y. Lei, L.P. Guo, B. Chen, I. Curosu, V. Mechtcherine, The connection between microscopic and macroscopic properties of ultra-high strength and ultra-high ductility cementitious composites (UHS-UHDCC), Compos. B Eng. 164 (2019) 144–157.
[32] Z. Lu, J. Yao, C.K. Leung, Using graphene oxide to strengthen the bond between PE fiber and matrix to improve the strain hardening behavior of SHCC, Cement Concr. Res. 126 (2019), 105899.
[33] Z. Zhang, A. Yuvaraj, J. Di, S. Qian, Matrix design of light weight, high strength, high ductility ECC, Construct. Build. Mater. 210 (2019) 188–197.
[34] Y. Li, X. Guan, C. Zhang, T. Liu, Development of high-strength and high-ductility ECC with saturated multiple cracking based on the flaw effect of coarse river sand, J. Mater. Civ. Eng. 32 (11) (2020), 04020317.
[35] H.H. Nguyễn, J.I. Choi, S.E. Park, S.L. Cha, J. Huh, B.Y. Lee, Autogenous healing of high strength engineered cementitious composites (ECC) using calcium-containing binders, Construct. Build. Mater. 265 (2020), 120857.
[36] Z. Zhang, F. Yang, J.C. Liu, S. Wang, Eco-friendly high strength, high ductility engineered cementitious composites (ECC) with substitution of fly ash by rice husk ash, Cement Concr. Res. 137 (2020), 106200.
[37] B.T. Huang, J.Q. Wu, J. Yu, J.G. Dai, C.K. Leung, V.C. Li, Seawater sea-sand engineered/strain-hardening cementitious composites (ECC/SHCC): assessment and modeling of crack characteristics, Cement Concr. Res. 140 (2021), 106292.
[38] Y. Yang, M.D. Lepech, E.H. Yang, V.C. Li, Autogenous healing of engineered cementitious composites under wet–dry cycles, Cement Concr. Res. 39 (5) (2009) 382–390.
[39] S.H. Chu, Effect of paste volume on fresh and hardened properties of concrete, Construct. Build. Mater. 218 (2019) 284–294.
[40] K. Wille, S. El-Tawil, A.E. Naaman, Properties of strain hardening ultra high performance fiber reinforced concrete (UHP-FRC) under direct tensile loading, Cement Concr. Compos. 48 (2014) 53–66.
[41] M.J. Kim, D.Y. Yoo, Y.S. Yoon, Effects of geometry and hybrid ratio of steel and polyethylene fibers on the mechanical performance of ultra-high-performance fiber-reinforced cementitious composites, J. Mater. Res. Technol. 8 (2) (2019) 1835–1848.
[42] X. Shen, E. Brühwiler, Influence of local fiber distribution on tensile behavior of strain hardening UHPFRC using NDT and DIC, Cement Concr. Res. 132 (2020), 106042.
[43] S.H. Chu, Development of Infilled Cementitious Composites, Composite Structures, 2021, 113885.
[44] J. Yu, Y. Chen, C.K. Leung, Mechanical performance of Strain-Hardening Cementitious Composites (SHCC) with hybrid polyvinyl alcohol and steel fibers, Compos. Struct. 226 (2019), 111198.
[45] Y. Zhou, B. Xi, K. Yu, L. Sui, F. Xing, Mechanical properties of hybrid ultra-high performance engineered cementitious composites incorporating steel and polyethylene fibers, Materials 11 (8) (2018) 1448.
[46] ASTM C1437, Standard Test Method for Flow of Hydraulic Cement Mortar, ASTM International, West Conshohocken, PA, 2020.
[47] M. Li, V.C. Li, Rheology, fiber dispersion, and robust properties of engineered cementitious composites, Mater. Struct. 46 (3) (2013) 405–420.
[48] ASTM C1856/C1856M, Standard Practice for Fabricating and Testing Specimens of Ultra-high Performance Concrete, ASTM International, West Conshohocken, PA, 2017.
[49] ASTM C109/C109M, Standard Test Method for Compressive Strength of Hydraulic Cement Mortars, ASTM International, West Conshohocken, PA, 2013.
[50] ASTM C469/C469M, Standard Test Method for Static Modulus of Elasticity and Poisson's Ratio of Concrete in Compression, ASTM International, West Conshohocken, PA, 2014.
[51] Japan Society of Civil Engineers, Recommendations for Design and Construction of High Performance Fiber Reinforced Cement Composites with Multiple Fine Cracks (HPFRCC), Concrete Engineering Series No, 2008, p. 82.
[52] B.T. Huang, Q.H. Li, S.L. Xu, C.F. Li, Development of reinforced ultra-high toughness cementitious composite permanent formwork: experimental study and digital image correlation analysis, Compos. Struct. 180 (2017) 892–903.
[53] B.T. Huang, J.G. Dai, K.F. Weng, J.X. Zhu, S.P. Shah, Flexural performance of UHPC-Concrete-ECC composite member reinforced by perforated steel plate, J. Struct. Eng. 147 (6) (2021), 04021065.
[54] J.G. Teng, Y. Xiang, T. Yu, Z. Fang, Development and mechanical behaviour of ultra-high-performance seawater sea-sand concrete, Adv. Struct. Eng. 22 (14) (2019) 3100–3120.
[55] B.T. Huang, Y.T. Wang, J.Q. Wu, J. Yu, J.G. Dai, C.K. Leung, Effect of fiber content on mechanical performance and cracking characteristics of ultra-high-performance seawater sea-sand concrete, Adv. Struct. Eng. 24 (6) (2020) 1182–1195.
[56] S.H. Chu, A.K.H. Kwan, A new bond model for reinforcing bars in steel fibre reinforced concrete, Cement Concr. Compos. 104 (2019), 103405.